

Timothy D. Burchell

Oak Ridge National Laboratory
Oak Ridge, Tennessee 37830-6088, USA

INTRODUCTION

During operation a graphite reactor core is subject to complex stresses which should not be sufficient to cause failure of the reactor core components. If safety margins are to be demonstrated, a credible and acceptable fracture model for graphite must be available, against which the probability of failure can be accurately predicted. A physically well-based model, which recognizes the dominant role of porosity in the graphite fracture process, has been described previously [1,2]. The successful application of the fracture model to H-451 graphite was also reported previously [3]. Here, we discuss a possible approach for applying the fracture model to describe the variation of tensile strength with neutron dose.

EXPERIMENTAL

The microstructural inputs required to model H-451 graphite, along with the experimental methods used to determine these inputs, are described elsewhere [3]. Irradiation effects data for grades H-451 and GraphNOL N3M graphites were obtained by irradiating specimens in target capsules in the High Flux Isotope Reactor (HFIR) at ORNL. Details of these experiments, and data for the neutron irradiation induced strength changes, have been published previously [4,5].

THEORETICAL FRACTURE MODEL

Detailed accounts of the fracture model are given elsewhere [1,2]. The model embodies the recommendations of Tucker et al. [6] who, in their review of graphite fracture, suggested the use of a fracture mechanics fracture criterion for particle fracture, and a microstructural approach to the fracture process. The model recognizes the key role of pores in the initiation of cracks when graphite is stressed. The failure criterion for a particle in the microstructure is shown in Fig. 1 where K_I is the stress intensity factor associated with an inherent defect (pore) of length c , K_I is the stress intensity factor associated with a plane in the particle at angle θ , and K_{Ic} is the particle stress intensity factor. It can be shown that the total probability of failure of a specimen or stressed volume is given by:

$$P_{tot} = [1 - \int f(c) \cdot P_f(\sigma,c) dc]^{2NV}$$

where $f(c)$ is the probability that a defect of length c exists in a log-normal distribution defined by a mean and standard deviation, $P_f(\sigma,c)$ is the probability that a defect of initial length c will propagate under stress σ to cause failure. N is the number of pores per unit volume and V is the specimen stressed volume. The following data are required to code the model for a specific

graphite: mean filler particle size, mean and standard deviation from a log-normal pore size distribution, and the density. Two pieces of specimen geometry specific data are required—the stressed volume and the specimen breadth. For a cylindrical specimen an equivalent breadth is calculated such that the specimen cross sectional area is identical.

RESULTS & DISCUSSION

Neutron irradiation induced changes in the strength of graphite can be differentiated into three stages (Fig. 2). In stage I a rapid increase in strength occurs due to dislocation pinning by irradiation induced defects such as lattice vacancies. This effect has typically saturated at doses <0.1 DPA. At greater neutron doses dimensional changes of the crystallites in the graphite cause shrinkage (densification), resulting in a further increase in strength (stage II). Figure 3 shows typical high dose dimensional change data for H-451 graphite from HFIR capsule HTK-7. The graphite initially shrinks, reaching a turn-around in volume at about 15-20 DPA. The initial shrinkage results from the "accommodation" of c-axis expansion by internal porosity allowing the a-axis shrinkage to dominate the dimensional change of the material. After turnaround, the graphite volume increases due to continued crystallographic c-axis expansion. During this phase of neutron damage, new porosity is created within the polygranular graphite due to the anisotropic crystallite dimensional changes. Consequently, the graphite is weakened by the introduction of new damaging porosity, and the strength gradually declines (stage III in Fig. 2). The close relationship between the volume and strength changes has been reported before [5] and is apparent from Figs. 2 and 3.

The microstructural parameters used in the fracture model will be affected by neutron irradiation. Data exist for the changes in volume (Fig. 3) and hence density of H-451 graphite, and these data are well described by binomial equations:

$$\begin{aligned} \text{Volume Change} &= 0.054 - 0.957D + 0.27D^2 \text{ and} \\ \text{Density Change} &= -0.072 + 1.027D - 0.03D^2 \end{aligned}$$

where d is the irradiation dose in DPA. Here, we assume the mean pore size of H-451 varies proportionally to the volume change calculated from the above equation. The pore area is assumed to change with dose as the square of the pore size. The number of pores is calculated from the total porosity (obtained from the density change) and the pore area. The final microstructural parameter that will vary significantly with neutron dose is the particle K_{Ic} . Several authors have reported that K_{Ic} increases on irradiation [7,8]. Here it is assumed that K_{Ic} increases rapidly upon irradiation, reaching a saturation value of $0.42 \text{ MN m}^{-3/2}$ at a dose of 0.1 DPA.

The microstructural input parameters were allowed to vary with neutron dose in the manner described above and for each dose increment the fractional change in the parameter calculated. The new inputs were then fed into the fracture model code and the mean tensile strength (50% failure probability) calculated. Figure 4 shows the calculated variation with neutron doses of K_{Ic} , pore size, pore area, number of pores, and porosity for H-451. Currently, experimental data are unavailable to confirm the precise nature of the variations of pore size, pore area, and the number of pores with neutron dose. However, one would expect the dependence assumed here to be at least qualitatively correct. Also shown in Fig. 4 is the calculated dose dependency of the mean strength. Clearly, stage I, II, and III behaviors, as described previously, are apparent in the model's predicted dose dependency of graphite strength.

CONCLUSIONS

A graphite fracture model has been applied to describe the neutron dose dependency of the strength of irradiated graphite. Certain assumptions were made regarding dose dependency of microstructural parameters. However, the predicted change of strength with increasing dose was qualitatively correct, showing an initial rapid increase in strength at very low dose, followed by a slowly increasing strength to a turnaround in the dose range 15-20 DPA. A much larger study of the effects of dose on graphite microstructure is required to fully elucidate the changes in pore structure.

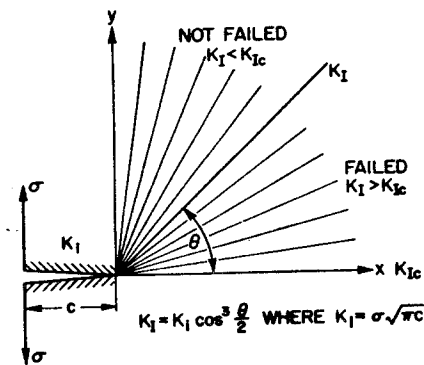


Fig. 1. Schematic illustration of the fracture criteria.

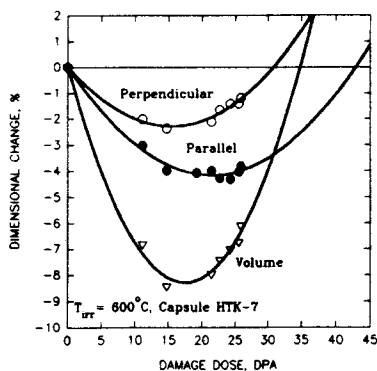


Fig. 3. Volume and dimensional changes of H-451 graphite.

REFERENCES

1. T. D. Burchell, "Studies of Fracture in Nuclear Graphite," Ph.D. Thesis, University of Bath, UK, 1986.
2. Proc. IAEA Specialist's Meeting on Status of Graphite Development for Gas Cooled Reactors, Toki-Mura Japan, Sept. 1991, IAEA TECDOC No. 690, Pub. IAEA, Vienna, Feb. 1993.
3. T. D. Burchell and J.P. Strizak, in *Proc 21st Bien.Conf. on Carbon*, p. 687, Pub. American Carbon Society, July 1993.
4. T.D. Burchell, JM Robbins, and J.P. Strizak, Report ORNL/NPR-91/35, Dec. 1991.
5. T. D. Burchell and W. P. Eatherly, *J. Nucl. Mat.*, **179-181** (1991) pp. 205-208.
6. M.O. Tucker, A.P.G. Rose, and T. D. Burchell, "The Fracture of Polygranular Graphite," *CARBON*, **24**, pp. 581-602, 1986.
7. S. Sato et al., *CARBON*, **27**, pp. 507-516, 1989.
8. W. Delle et al., in *Proc Carbon '88*, pp. 446-448, Pub. Inst. of Physics, London 1988.

This Research was sponsored by the office of Nuclear Energy, U.S. Department of Energy, under contract DE-AC05-84OR 21400 with Martin Marietta Energy Systems, Inc.

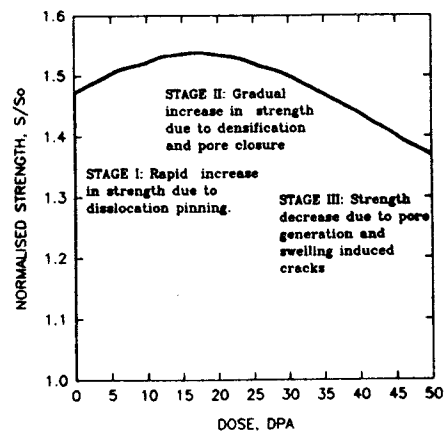


Fig. 2. The effects of neutron dose on graphite strength.

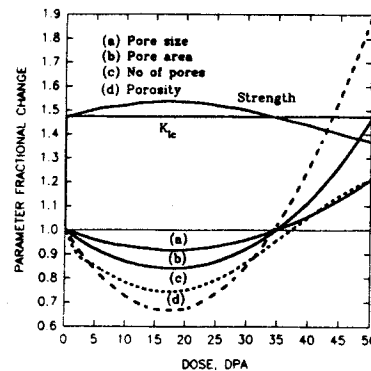


Fig. 4. The variation of microstructural parameters with dose and the predicted strength dependency.